Tracking the reasons for the peculiarity of Cr/Al_2O_3 catalyst in ethylene polymerization.

Giorgia A. Martino[1], Caterina Barzan[1], Alessandro Piovano[1], Andriy Budnyk[1,2] and Elena Groppo[1]*

[1]*University of Torino, Department of Chemistry, NIS Centre and INSTM, Via G. Quarello 15A, I10135, Italy.*

[2]*Southern Federal University, International Research Center "Smart Materials", Zorge 5, Rostov-on-Don, 344000, Russia*

*Corresponding author: elena.groppo@unito.it

Abstract

Looking to the past, heading to the future. In this contribution we explain the reasons why the Cr/Al_2O_3 Phillips catalysts exhibit a faster kinetics profile in ethylene polymerization reaction with respect to Cr/SiO_2. Diffuse reflectance UV-Vis and FT-IR spectroscopies unequivocally demonstrate that, albeit several types of reduced Cr sites are stabilized by the Al_2O_3 support, only the 4-fold coordinated Cr^{2+} sites are active precursors in ethylene polymerization, as for Cr^{2+}/SiO_2. Nevertheless, kinetic experiments indicate that ethylene polymerization is 15 times faster on CO-reduced Cr/Al_2O_3 than on CO-reduced Cr/SiO_2. The difference is even more striking (two order of magnitude) when the reaction rates per active Cr sites are compared. Our experimental results suggest two reasons behind the faster polymerization kinetic of Cr/Al_2O_3: 1) the higher ionic character of the Cr-O-Al bond with respect to the Cr-O-Si one; 2) the nature of the ancillary ligands in the coordination sphere of the Cr active sites (which are mainly carbonates for CO-reduced Cr/Al_2O_3 and siloxane bridges for CO-reduced Cr/SiO_2).

Keywords: chromium, alumina, ethylene polymerization, ancillary ligands, FT-IR spectroscopy, UV-Vis-NIR spectroscopy

1. Introduction

The Cr-based Phillips catalyst is among the most important heterogeneous catalysts for ethylene polymerization. It accounts for about 50% of the high density polyethylene (HDPE) world's demand, owning also a large share of linear low density polyethylene (LLDPE) market [1-3]. Generally speaking, the active phase is constituted by a highly dispersed chromium oxide supported on a high surface area material [4]. Porous silica has been traditionally employed, due to its tendency to fragment during the polymer growing. The smaller silica fragments generated in this process provide new chromium sites accessible for ethylene polymerization. Besides silica, almost all the high surface area oxides have been tested as supports, and some of them also found practical applications [5-9]. In this context, also alumina (Al_2O_3) was tested, but the resulting Cr/Al_2O_3 catalyst was left aside due to its tendency to fast deactivation, providing only 10-20% of the polymerization activity of Cr/SiO_2. Noticeably, alumina does not fulfil the fragility, porosity and high surface area standards required for boosting polymerization. Nevertheless, the Cr/Al_2O_3 catalysts do show some unique features compared to Cr/SiO_2, that could make them extremely appealing [5]: 1) a much faster kinetic profile (i.e. rapid development of polymerization upon ethylene addition); 2) a lower tendency to β-hydride elimination (the polyethylene produced in the absence of H_2 has an extremely high molecular weight, approaching the ultra-high classification); 3) an unusual tendency to distribute the branching evenly throughout the molecular weight distribution (nearly all the physical properties of the polymer are improved); 4) a much higher H_2 sensitivity as chain transfer agent (which implies the possibility of controlling the molecular weight distribution). The reasons behind these peculiar features must be searched in the molecular structure of the Cr sites.

The singular properties of Cr/Al_2O_3 stimulated us to carry out a complete spectroscopic investigation at a molecular level of the Cr sites, aimed at tracking the reasons behind the unusual features of Cr/Al_2O_3 in ethylene polymerization. The literature on the spectroscopic properties of Cr^{6+}/Al_2O_3 is wide, since this is one of the most used catalysts for propene dehydrogenation [10-25]. Opposite to the case of Cr^{6+}/SiO_2, for which the aggregation state and the structure of the grafted Cr^{6+} sites is still debated [5, 7-9, 20, 22-24, 26-35], there is a general consensus on that Cr^{6+} on Al_2O_3 exists primarily as (tetrahedrally coordinated) monochromate species [9, 19-24, 36]. Much less was done on reduced Cr/Al_2O_3, and the reference works remain those of Weckhuysen et al. dating back to the middle of 1990s [9, 19-24, 36]. More recently, Airaksinen et al. [25] studied the reduction of alumina-supported chromia containing 13 wt.% chromium, by X-ray photoelectron and absorption

spectroscopies, in situ temperature-programmed Raman and diffuse reflectance FT-IR spectroscopies, combined with mass spectrometry. According to these seminal works, after reduction by carbon monoxide or hydrogen mainly Cr^{3+} is formed, although the formation of Cr^{2+} in carbon monoxide reduction was also observed. In the last years spectroscopic methods have progressed enormously. For this reason, it is timely a systematic spectroscopic investigation on reduced Cr/Al_2O_3 catalysts, with the specific purpose to determine the structure of the reduced Cr sites and to correlate it with its unusual behaviour in ethylene polymerization with respect to Cr/SiO_2. Both H_2 and CO have been used as reducing agents as indicated by the literature [5]. Transmission FT-IR and Diffuse Reflectance UV-Vis-NIR spectroscopies coupled with molecular probes have been employed to confirm the presence of different Cr reduced species at the catalyst surface and to clarify which are those involved in the ethylene polymerization reaction.

2. Experimental Section

2.1 Materials.

The alumina-supported Phillips catalysts were prepared by wet-impregnation, using as a support a transition-Al_2O_3 (Aeroxide Alu C, Evonik-Degussa) characterized by a specific surface area of 100 m^2/g, and CrO_3 (Sigma-Aldrich) as Cr precursor, according to the procedure already adopted for the synthesis of Cr/SiO_2 [8]. Two Cr/Al_2O_3 samples differing in the Cr loading (1 wt% and 0.5 wt%, hereafter referred to as $0.5Cr/Al_2O_3$ and $1.0Cr/Al_2O_3$, respectively) were prepared: the former was used for the FT-IR measurement and the latter for DR-UV-Vis-NIR and kinetics experiments. The choice was done to optimize the spectral quality. Cross-checking experiments demonstrated that the spectroscopic properties are the same irrespective of the Cr loading, as already demonstrated in the past for the similar Cr/SiO_2 catalyst [8].

The catalysts were activated directly inside the measurement cells, that can be connected to a vacuum line allowing activations and gas dosages. The activation procedure was very similar to that well optimized for Cr/SiO_2 catalysts [8]. Briefly, the main steps are: i) degassing in dynamic vacuum at increasing temperature up to 650 °C to dehydroxylate the alumina surface; ii) oxidation at the same temperature in the presence of O_2, resulting in the grafting of the Cr species at the alumina surface; iii) reduction in the presence of CO or H_2 at 350 °C, followed by removal of the gaseous phase at the same temperature; iv) cooling down at room temperature. For probing the accessible Cr sites, CO was dosed at room temperature (equilibrium pressure P_{CO} = 100 mbar), followed by step-by-step expansions. The kinetics of ethylene polymerisation was studied by

sending 200 mbar of ethylene at room temperature over 0.5 grams of catalyst inside a quartz reactor of known volume, and recording the ethylene pressure as a function of time. Similar experiments were repeated for the catalyst inside the FT-IR and DR UV-Vis cells, collecting the spectra as a function of time.

2.2 Methods.

Transmission FT-IR spectra were collected at 2 cm^{-1} resolution with a Bruker Vertex70 instrument equipped with a MCT detector. The experiments were performed in situ and in controlled atmosphere within a quartz cell equipped with two KBr windows, allowing performing thermal treatments and measurements in the presence of gases. The FT-IR spectra were normalized to the optical thickness of the pellet.

Diffuse reflectance (DR) UV-Vis-NIR spectra were collected using a Varian Cary5000 spectrophotometer with a diffuse reflectance accessory. The samples were measured in the powder form, inside a cell made of optical quartz, allowing performing thermal treatments and measurements in the presence of gases. The reflectance (%R) signal was later converted into Kubelka-Munk values.

3. Results and discussion

3.1 The role of CO and H_2 as reducing agents for Cr^{6+}/Al_2O_3

The spectroscopic properties of Cr^{6+} on Al_2O_3 are well known in the specialized literature. While for Cr^{6+} on SiO_2 there is still a debate on the aggregation state of the Cr^{6+} species (both mono- and dichromates have been proposed [5, 7-9, 20, 22-24, 26, 34, 35], or even mono-oxo CrO_5 [27-33]), Cr^{6+} exist primarily as monochromate species on Al_2O_3 [9, 19-24, 36] (the corresponding DR UV-Vis-NIR spectrum is shown in Figure S1a). Temperature-programmed reduction measurements have demonstrated that Cr^{6+} on Al_2O_3 are more reducible than Cr^{6+} on SiO_2 (i.e. their reduction is achieved at lower temperature), both in CO and in H_2 [5, 37]. DR UV-Vis-NIR spectroscopy has been traditionally used to determine the final valence state of the reduced Cr sites in Cr/Al_2O_3, Cr/SiO_2 and variant thereof [8, 9, 19-24, 36-41]. Although DR UV-Vis-NIR is often disused in favour of other methods (such as XANES or EPR), it remains one of the techniques most informative on the electronic properties of heterogeneous catalysts. In the specific case of Cr^{n+} sites on inorganic support, the literature on the topic is well assessed. DR UV-Vis-NIR spectroscopy has been used since the early 1990s not only to discriminate among various oxidation states and coordination geometries, but also to quantify the amount of each species as a function of the sample

composition and treatment. For this reason, we started our investigation by collecting the DR UV-Vis-NIR spectra of Cr/Al$_2$O$_3$ reduced in CO and in H$_2$ at 350 °C (Figure 1, spectra 1 and 1', respectively).

The DR UV-Vis-NIR spectra demonstrate that in the adopted experimental conditions most of the Cr^{6+} species have been reduced in both cases. Indeed, the intense charge-transfer band at 27000 cm^{-1} characteristic of mono-chromates [9, 19-24, 36, 42] is no longer observed. Both spectra are dominated by an intense band centred at 39000 cm^{-1}, which is straightforwardly assigned to an oxygen to chromium (O → Cr) charge transfer transition [9, 19-24, 36, 43, 44]. In the low wavenumbers region, a multitude of bands are observed and assigned to d-d transitions of several types of reduced Cr sites, differing in the oxidation state and coordination geometry. In particular, a very broad envelop of d-d bands is observed in the spectrum of the CO-reduced catalyst, while that of the H$_2$-reduced catalyst displays more defined bands centred at 26000, 16000 and 10500 cm^{-1}. The presence of a multitude of d-d bands suggests a larger heterogeneity of reduced Cr sites with respect of those obtained on Cr/SiO$_2$ systems [8], comprising both +3 and +2 oxidation states and different coordination geometries. It is worth noticing that the spectrum of the CO-reduced catalyst is comparable to those previously reported by Weckhuysen et al. for similar systems [9, 19-24, 36], which are unanimously considered as the reference spectra in this field.
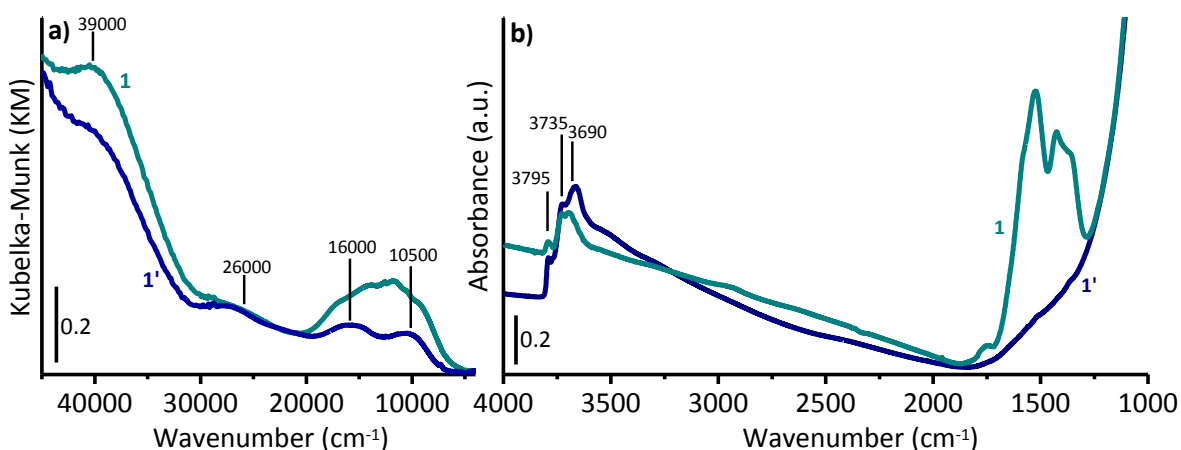

Figure 1 Part a) DR UV-Vis-NIR of the 0.5Cr/Al$_2$O$_3$ catalyst reduced in CO at 350 °C (curves 1) and in H$_2$ at 350 °C (curves 1'). Part b) FT-IR spectra of the 1.0Cr/Al$_2$O$_3$ catalyst reduced in CO at 350 °C (curves 1) and in H$_2$ at 350 °C (curves 1'). The FT-IR spectra are normalized to the thickness of the pellet.

The assignment of the d-d bands is straightforward on the basis of the specialized literature [9, 19-24, 36]. The UV-Vis spectra of 6-fold coordinated Cr^{3+} species (Cr$^{3+}_{6c}$) are expected to show

two equally intense d-d bands centred at around 17000 cm^{-1} ($^4A_{2g} \rightarrow {}^4T_{2g}$ transition) and 25000 cm^{-1} ($^4A_{2g} \rightarrow {}^4T_{1g}$ transition) and a third one, rather weak, at 37000 cm^{-1} (which is however always masked by the intense charge-transfer band at high energy) [20, 23, 45]. On the other hand, the spectra of undistorted 6-fold coordinated Cr^{2+} ions (Cr$^{2+}_{6c}$) in high-spin 3d^4 complexes are known to show a single d-d band centred between ca. 10000 and 20000 cm^{-1}, which is ascribed to the $^5E_g \rightarrow {}^5T_{2g}$ transition [45]. For example, the hexa-aquo Cr^{2+}(H$_2$O)$_6$ complex shows a single transition around ca. 14000 cm^{-1} [45]. The DR UV-Vis-NIR spectra of the two reduced Cr/Al$_2$O$_3$ catalysts are characterized by bands around 26000 and 16000 cm^{-1}, which are compatible with the presence of both Cr$^{3+}_{6c}$ and Cr$^{2+}_{6c}$ species. However, in both cases an additional d-d band is observed around 10500 cm^{-1}, that univocally demonstrates the presence of Cr^{2+} species in a lower symmetry. Indeed, bands at wavenumbers as low as 10000 cm^{-1} have been reported since 1960s for several distorted tetrahedral complexes of Cr^{2+} [46-48], and are commonly observed in the UV-Vis spectra of the CO-reduced Cr/SiO$_2$ catalysts, where 4-fold (pseudo-tetrahedral) coordinated Cr^{2+} sites (Cr$^{2+}_{4c}$) are cleanly and selectively obtained.

On these basis, the DR UV-Vis-NIR spectra in Figure 1 allow concluding that the reduction of Cr^{6+}/Al$_2$O$_3$ catalyst leads to the formation of at least three types of reduced chromium sites, differing in the oxidation state and coordination geometry, in close agreement with the seminal works of Weckhuysen et al. [9, 19-24, 36]. The relative concentration of the Cr$^{2+}_{4c}$, Cr$^{2+}_{6c}$ and Cr$^{3+}_{6c}$ sites is a function of the reduction conditions and can be roughly estimated by deconvolving the DR UV-Vis-NIR spectra in the d-d region with four Gaussian curves centred at ca. 10500, 14000, 16000 and 26000 cm^{-1} (Figure S2), and considering that the molar extinction coefficient of spin-allowed/Laporte partially allowed (by p-d mixing) transitions (as for tetrahedral complexes) is usually ten times larger than that of spin-allowed/Laporte forbidden transitions (as for octahedral complexes) [45, 49]. We found that reduction in H$_2$ at 350 °C leads to the preferential formation of Cr$^{3+}_{6c}$ sites (ca. 98 %), with a small amount of Cr$^{2+}_{4c}$ species (ca. 2 %). Whereas reduction in CO at the same temperature leads to a larger heterogeneity of sites, with Cr$^{3+}_{6c}$, Cr$^{2+}_{6c}$, Cr$^{2+}_{4c}$ sites accounting for about 70%, 22% and 8% of the total, respectively.

The preferential formation of Cr$^{3+}_{6c}$ species differentiates Cr/Al$_2$O$_3$ from Cr/SiO$_2$, where mainly Cr$^{2+}_{4c}$ species are formed upon reduction in CO and only a small amount of Cr$^{3+}_{6c}$ species are obtained after reduction in H$_2$ [8, 33, 50]. This difference has been explained by Weckhuysen et al. [23] considering the different "hardness" of the two supports, where a harder support – according to the definition first introduced by Pearson [51] – means that it is less susceptible to electron

fluctuations [52]. Silica is "softer" and this facilitates the reduction of Cr^{6+} in Cr^{2+}, whereas alumina is "harder" and retards the reduction (leading to Cr^{3+} formation) [9]. Moreover, the so formed Cr^{3+} species are quite stable on the alumina surface because of the similarity in size and charge with Al^{3+} ($r(Cr^{3+}_{Oh}) = 0.615$ Å and $r(Al^{3+}_{Oh}) = 0.53$ Å) [53], that makes relatively easy to diffuse into vacant octahedral Al^{3+} sites. The Cr^{3+} sites occupying the octahedral interstices in the Al_2O_3 lattice are clearly not accessible to incoming molecules. A similar structure is believed for Cr^{2+}_{6c}, whose formation implies a slight distortion of the crystalline structure because of the bigger dimension of the Cr^{2+} ions. On the other hand, the 4-fold coordinated Cr^{2+} sites stay on the surface, covalently bonded to the alumina through two oxygen atoms and with two other additional weaker ligands in the coordination sphere, in analogy to the Cr/SiO_2 catalyst.

The FT-IR spectra of the reduced Cr/Al_2O_3 catalysts (Figure 1b) are dominated by the intense (and out of scale) absorption due to the vibrational modes of the framework (below 1200 cm^{-1}) and by several weak absorption bands in the 3800-3500 cm^{-1} region (with maxima at 3795, 3735, 3690 cm^{-1}), due to the ν(OH) modes of various surface OH groups. The large amount of surface OH groups characterized by a slightly different acidity [54-62] in contrast with the presence of isolated, well-defined, silanol groups at the SiO_2 surface, is a direct consequence of the Lewis acidity of Al_2O_3 [54, 55]. The higher intensity of the ν(OH) bands in the spectrum of the H_2-reduced catalyst indicates a larger amount of OH species. This was already reported in the literature [25] and is expected, since the by-product of chromates reduction is water that, at 350 °C, partially re-hydrates the silica surface. On the other side, the spectrum of the CO-reduced catalyst shows a series of broad absorption bands in the 1800 − 1100 cm^{-1} region which have been attributed in the specialized literature to pseudo-carbonate species [25, 56, 63-66]. The presence of these species is a direct consequence of the tendency of some metal oxides (including alumina) to reactively adsorb CO_2 on their basic surface sites with the consequent formation of different kinds of carbonates [67]. In the present case, CO_2 is produced in situ during the reduction of the chromate species in CO at 350 °C. This is observed also for reduction of Cr^{6+}/SiO_2 in CO [66, 68], although the absence of basic sites at the silica surface allows for a complete removal of CO_2 at the reduction temperature [8]. Interestingly, a small amount of surface carbonates are also formed when pure Al_2O_3 is treated in the same conditions (Figure S2), indicating that a surface reduction occurs at some extent, although alumina is usually considered a not reducible metal-oxide. The process likely involves the formation of oxygen vacancies on a few defective sites.

3.2 Accessibility of the reduced Cr sites

The abundant literature on Cr/SiO$_2$ catalysts demonstrates that CO is an excellent molecular probe for reduced chromium species [8, 9, 69]. Figure 2 shows the evolution of the DR UV-Vis-NIR and FT-IR spectra of CO- and H$_2$-reduced Cr/Al$_2$O$_3$ catalysts as a function of the CO coverage at room temperature. The DR UV-Vis-NIR spectra of both catalysts change in the presence of CO (spectra 2 and 2' in Figure 2ac) mainly in the d-d region. In particular, the absorption bands attributed to Cr$^{2+}_{4c}$ originally at around 10000 cm^{-1} drastically decreases in intensity, while simultaneously a new band appears around 15000 cm^{-1} typical of Cr$^{2+}_{6c}$ species. The phenomenon is more evident when looking to the difference spectra (Figure S4). The presence of an isosbestic point at ca. 13000 cm^{-1} indicates that the Cr$^{2+}_{4c}$ species are converted into Cr$^{2+}_{6c}$ species, due to CO coordination [8]. The weaker intensity of the newly formed band is in agreement with the expected lower extinction coefficient for transitions involving 6-fold coordinated sites [45]. Upon degassing CO, the original spectra are restored, indicating that CO adsorption on Cr$^{2+}_{4c}$ sites is a reversible process. On the other hand, the bands attributed to Cr$^{2+}_{6c}$ and Cr$^{3+}_{6c}$ sites are not influenced by the presence of CO, unequivocally demonstrating that these sites are mostly inaccessible to the CO molecule, as expected since their coordination sphere is fully occupied. Supplementary experiments of re-oxidation in the presence of O$_2$ (Figure S5) verified that all the reduced Cr sites are re-oxidized to Cr^{6+}, thus excluding that Cr$^{3+}_{6c}$ and Cr$^{2+}_{6c}$ are completely buried in the Al$_2$O$_3$ lattice. It is worth noticing that the spectroscopic behaviour is the same whether or not carbonates are present at the catalyst surface.
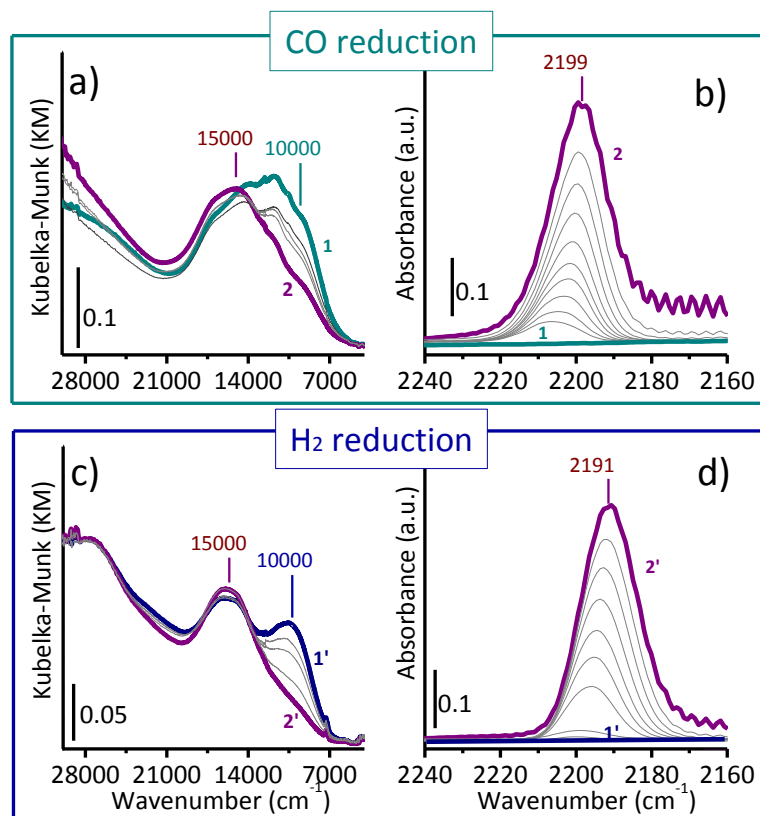
Figure 2: Part a) DR UV-Vis-NIR spectra in the d-d region of the CO-reduced 0.5Cr/Al$_2$O$_3$ catalyst (spectrum 1), and of the same sample in the presence of CO (P$_{CO}$ = 100 mbar) at room temperature (spectrum 2). Grey spectra show the effect of gradual CO desorption at room temperature. Part b) Evolution of the FT-IR spectra (magnification of the ν(CO) region) upon CO adsorption at room temperature on the CO-reduced 1.0Cr/Al$_2$O$_3$ catalyst as a function of P$_{CO}$ coverage, from P$_{CO}$ = 100 mbar (spectrum 2) to zero (spectrum 1). Parts b) and d): as part a) and c) for H$_2$-reduced 0.5Cr/Al$_2$O$_3$ and 1.0Cr/Al$_2$O$_3$, respectively.

Figure 2bd show the FT-IR spectra, in the ν(CO) region, of CO adsorbed on the two catalysts as a function of the CO coverage. At the maximum coverage, the spectra are dominated by an intense and quite broad absorption band, centered at 2199 cm^{-1} for CO-reduced Cr/Al$_2$O$_3$ and at 2191 cm^{-1} for H$_2$-reduced Cr/Al$_2$O$_3$. The observation of a single (although broad) absorption band for all the CO coverage indicates the formation of mono-carbonyl Cr complexes. This differentiates again reduced Cr/Al$_2$O$_3$ from Cr^{2+}/SiO$_2$, where a fraction of very low-coordinated Cr^{2+} sites are able to adsorb up to two CO molecule in the same experimental conditions [8]. In principle, both Cr^{n+} and surface Al^{3+} sites could be available for CO adsorption. CO adsorbed on unsaturated Al^{3+} sites has been reported to contribute in this wavenumber region, but with very weak bands at room temperature [56, 70], opposite to what observed herein. Hence, both bands observed in Figure 2bd are ascribed to mono-carbonyl adducts formed on reduced Cr sites. The shift of the ν(CO) bands at

9

higher frequencies upon decreasing the CO coverage, observed in both cases, reveals the occurrence of inter-molecular interactions between CO molecules adsorbed nearby. This phenomenon is typically observed on ordered surfaces [69-73]. In the present case, it might reflect the proximity of several available adsorption sites for CO, comprising not only the reduced Cr sites, where CO is strongly bonded, but also the unsaturated Al^{3+} sites.

The position of both bands indicates that the interaction of CO with the reduced Cr sites is dominated by σ-donation/polarization effects, while π-back donation is negligible. Similar "non classic" carbonyls are formed on Cr^{2+}/SiO_2, which account for v(CO) bands around 2180 cm^{-1} [8]. The much higher v(CO) values observed for CO adsorbed on Cr/Al_2O_3 reduced in CO and in H_2 (+10 and +20 cm^{-1}, respectively) could be attributed, in principle, to a higher oxidation state of the accessible Cr sites. For instance, bands at very similar v(CO) values (2188 and 2202 cm^{-1}) were assigned by Copéret et al. [74] to CO adsorbed on well-defined Cr^{3+} sites at the silica surface. However, in our case the DR UV-Vis results discussed above unequivocally show that only the Cr^{2+}_{4c} sites are accessible to CO at room temperature. Hence, the absorption band in Figure 2bd is attributed to mono-carbonyl adducts formed on Cr^{2+}_{4c} sites. The position of the v(CO) band can be explained by considering the more ionic character of alumina with respect to silica. Indeed, according to Busca [54, 55, 58], semi-metal oxides, such as silicas, are constituted by essentially covalent network structures (i.e. the Si-O bond is classifiable as a covalent bond), while typical metal oxides (such as titania, zirconia, and alumina) are essentially ionic network structures (i.e. the Al-O bond has the characteristics of an ionic bond). Hence, a Cr^{2+} site grafted at the alumina surface feels a lower electronic density than a Cr^{2+} site at the surface of silica, because of the more ionic character of the Al–O bond with respect to the Si–O bond. The difference in 10 cm^{-1} observed in the position of the v(CO) absorption bands for the two catalysts can be explained by considering the different local environment of the Cr^{2+}_{4c} sites in CO- and H_2-reduced Cr/Al_2O_3. Indeed, in the H_2-reduced sample a fraction of the Cr^{2+}_{4c} sites might be partially in interaction with surface –OH groups, which are by far more abundant than in the CO-reduced sample (Figure 1b). In the CO-reduced sample, at least a fraction of the Cr^{2+}_{4c} sites are in proximity of surface carbonates (Figure 1b), i.e. of electronegative groups. A similar induction effect was reported in the early 1990s for CO adsorbed on Cr_2O_3 in the presence of carbonates [75]. In this respect, it is worth noticing that CO adsorption on CO-reduced Cr/Al_2O_3 causes a perturbation of the absorption bands associated to surface carbonates-like species (Figure S6), which is largely reversible upon decreasing the CO pressure.

Summarizing, in contrast to the Cr^{2+}_{4c} sites present at the surface of the CO- reduced Cr^{2+}/SiO_2 catalyst (where the ancillary ligands are, at most, the strained siloxane bridges), the CO- and H_2- reduced Cr/Al_2O_3 catalysts display accessible surface Cr^{2+}_{4c} sites at least partially surrounded by carbonates and hydroxyl groups, respectively. The presence of these ancillary ligands might influence the reactivity of the reduced Cr/Al_2O_3 catalysts towards ethylene.

3.3 Ethylene polymerisation

Kinetic experiments were performed on both the CO- and H_2-reduced Cr/Al_2O_3 catalysts to evaluate the ethylene polymerization rate in comparison with the CO-reduced Cr^{2+}/SiO_2 catalyst [76, 77]. Figure 3a shows the decrease of ethylene pressure as a function of time for the three catalysts, monitored in the same experimental conditions and at a constant Cr loading. The data indicate that the CO-reduced Cr/Al_2O_3 catalyst is almost 15 times faster than the Cr^{2+}/SiO_2 catalyst and even 350 times faster than the H_2-reduced Cr/Al_2O_3 catalyst. The ethylene polymerization rate observed for the Cr/Al_2O_3 catalyst reduced in CO is in good agreement with the "fast kinetics" of the chromia alumina reported by McDaniel [5]. By plotting the $lnP(C_2H_4)$ versus time (that is, under the usual approximation of a first-order reaction), rate constants of 0.6 and 210 $s^{-1}molCr^{-1}$ were obtained for H_2- and CO-reduced Cr/Al_2O_3, to be compared with the value of 15 $s^{-1}molCr^{-1}$ obtained for Cr/SiO_2 in the same reaction conditions [78].

In situ time-resolved FT-IR spectroscopy is in qualitative agreement with the kinetic experiments. Figures 3bc show the time-resolved FT-IR spectra collected during ethylene polymerization (P_{C2H4} = 100 mbar) at room temperature on both the CO- and H_2-reduced Cr/Al_2O_3 catalysts. The occurrence of ethylene polymerization is indicated by the growth of the IR absorption bands characteristic of polyethylene, in both $\nu(CH_2)$ and $\delta(CH_2)$ vibrational ranges (at 3000-2800 and 1500-1350 cm^{-1}, respectively). The much faster ethylene polymerization rate of CO-reduced Cr/Al_2O_3 is demonstrated by the rapid saturation of the $\nu(CH_2)$ absorption bands (after 35 seconds only), while the same bands reach a lower intensity even after 30 minutes of ethylene reaction on H_2-reduced Cr/Al_2O_3 (lower amount of polyethylene formed).

Additional information can be obtained by a closer inspection of the FT-IR spectra in Figure 3bc: 1) the formed polyethylene is highly crystalline also at short polymerization time, as evidenced by the intensity ratio between the two $\delta(CH_2)$ bands at 1472 and 1463 cm^{-1} [79]; 2) the absorption bands assigned to surface pseudo-carbonates in the spectrum of the CO-reduced catalyst are slightly perturbed immediately after ethylene dosage (inset in Figure 3b). The effect is similar to

that observed in the presence of CO, validating the previous conclusion on the close proximity of carbonates to a fraction of the reduced Cr^{2+}_{4c} sites; 3) at long polymerization time, i.e. for high polyethylene content, also the $\nu(OH)$ bands are perturbed, as a consequence of the interaction with the polyethylene chains [8].

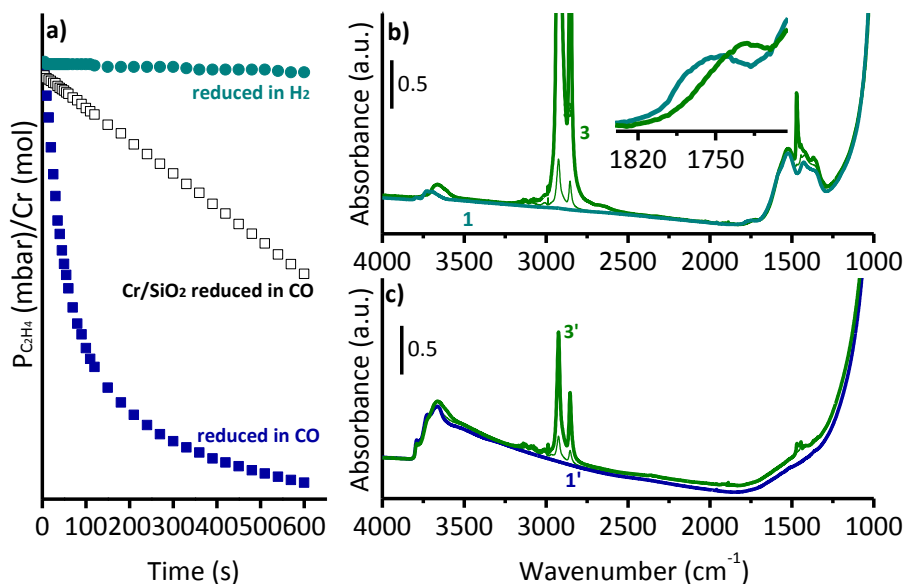**Figure 3** Part a) Kinetics of ethylene polymerisation on CO- and H_2-reduced $1.0Cr/Al_2O_3$ catalysts, compared to that of CO-reduced Cr/SiO_2 obtained by recording the ethylene pressure as a function of time. Parts b) and c) Time resolved FT-IR spectra collected during the C_2H_4 polymerization at room temperature on the $1.0Cr/Al_2O_3$ catalyst reduced in CO after 35 seconds of polymerization (spectrum 3) and on the same catalyst reduced in H_2 after 30 minutes of polymerization (spectrum 3'), respectively. Grey spectra are collected at intermediate times. The inset in part b) shows a magnification of the spectral region where only the carbonates contribute, to highlight the effect of ethylene polymerization on the absorption bands ascribed to carbonates.

In order to understand which reduced Cr site is active in ethylene polymerization, we followed the reaction at room temperature by means of DR UV-Vis-NIR spectroscopy on both the CO- and H_2-reduced Cr/Al_2O_3 catalysts. The resulting spectra are shown in Figure 4. Upon ethylene dosage, the DR UV-Vis-NIR spectra of both catalysts change mainly in the d-d region, where the d-d bands previously ascribed to Cr^{2+}_{4c} sites are gradually eroded (see arrows in Figure 4). Meanwhile, weak bands grow in the 4500-4000 cm^{-1} region, where overtones and combinations of the stretching and bending vibrational modes of polyethylene are located (see insets in Figure 4). These results provide a strong evidence that the Cr^{2+}_{4c} sites are those mainly involved in ethylene polymerization, whereas the other reduced chromium species (Cr^{2+}_{6c} and to Cr^{3+}_{6c} sites) are mostly

inactive, because inaccessible to ethylene (as for CO, Figure 2). Interestingly, the disappearance of the spectroscopic fingerprints of Cr^{2+}_{4c} is not accompanied by the appearance of any additional band that could reveal the destiny of the active sites. Likely, the Cr active sites remain buried into a layer of polyethylene and become rapidly invisible to DR UV-Vis-NIR. This is a limitation intrinsic to the physical method with which the UV-Vis spectra are collected. Indeed, in the reflectance mode, the spectrophotometer collects the light scattered by the sample. As soon as a coating of polyethylene is formed around the Cr/Al_2O_3 particles, their size rapidly approaches the nanometer range, and they become strong light scatterers, thus preventing the light from penetrating deeply into the sample (i.e. where there are the Cr sites). This is macroscopically visible in the aspect of the sample that progressively becomes white. The white colour is not the colour of polyethylene (which is transparent in the whole UV-Vis region), neither that of Cr/Al_2O_3 (whichever is the oxidation state, Cr ions give always a colour different than white). Rather, the white colour is the result of the scattering of the light from the combination polyethylene + catalyst particles. In these conditions, no information on the active Cr sites can be obtained anymore. However, collecting the UV-Vis spectra in the early stages of ethylene polymerization allows following the process. The first spectroscopic manifestation of Cr/Al_2O_3 that disappear during the formation of polyethylene are those associated to the active sites (i.e. where the polymer is forming).

The results summarized above converge in indicating that, in our experimental conditions, the 4-fold coordinated Cr^{2+} sites are those acting as precursors in ethylene polymerization, although we cannot solve (for the moment) the long-standing question about the mechanism of ethylene polymerization [76, 80-82]. This is in agreement with a part of the specialized literature (citing Max McDaniel, Cr(II) is at least an active precursor, but whether the chromium remains divalent during olefin polymerization is doubtful [5]). This statement does not exclude that also Cr^{3+} sites may be active in ethylene polymerization to some extent, as for ad-hoc synthesized catalytic systems reported in recent literature [74, 83, 84].

Once determined which are the Cr sites mainly involved in the ethylene polymerization reaction (Cr^{2+}_{4c}) and knowing their approximate concentration (as assessed by DR UV-Vis-NIR spectroscopy), it is possible to estimate the reaction rates per active site. Values of 30 and 2625 $s^{-1}[mol(Cr^{2+}_{4c})]^{-1}$ have been obtained for H_2- and CO-reduced Cr/Al_2O_3, to be compared with 15 $s^{-1}molCr^{-1}$ of Cr/SiO_2 (since the totality of Cr sites in Cr/SiO_2 are Cr^{2+}_{4c}). Although approximated, these values clearly indicate that Cr^{2+}_{4c} sites on Al_2O_3 are intrinsically more active than the same sites on SiO_2 (effect of the support). Moreover, the Cr^{2+}_{4c} sites on CO-reduced Cr/Al_2O_3 are ca. two orders of

magnitude more active than those on H_2-reduced Cr/Al_2O_3 (effect of the ancillary ligands). It emerges that both the electronic and the local structure of the chromium sites play a major role in affecting their catalytic performances. The support is decisive in influencing both properties, but also the preparation and activation steps are important instruments to tune the properties of the Cr active sites. This explains why, at the present, there is still a controversy on the oxidation state of the active Cr sites. Considering all the variables in the catalyst synthesis and activation, we believe that the two main hypothesis (+2 and +3) may coexist.
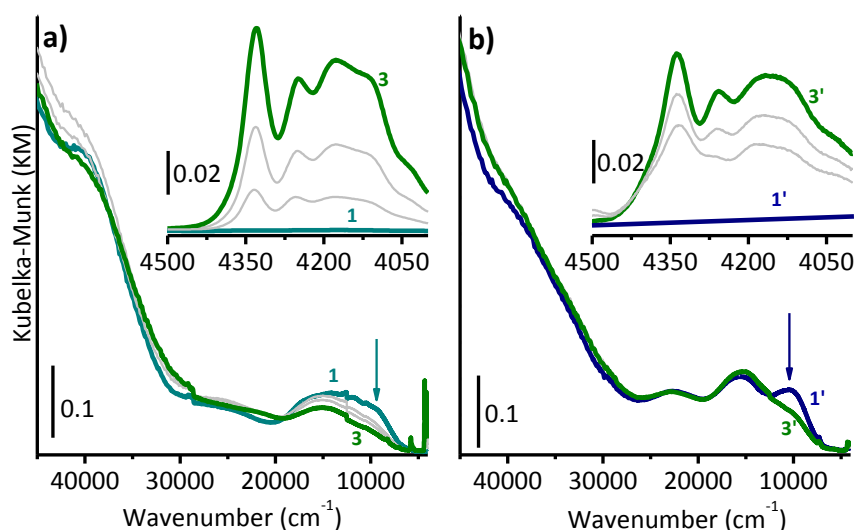
Figure 4 Part a): DR UV-Vis-NIR spectrum of $0.5Cr/Al_2O_3$ reduced in CO at 350°C (spectrum 1) and during ethylene polymerization at room temperature (grey); the last spectrum (spectrum 3) is collected at the end of the reaction. The arrow highlights the band more affected by ethylene polymerization. The inset shows a magnification in the region where the combination of polyethylene stretching and bending modes are observable. Part b): as part a) for the $0.5Cr/Al_2O_3$ reduced in H_2 at 350°C.

4. Conclusions

In this work we thoroughly investigated the physical-chemical properties of the Cr/Al_2O_3 catalyst, aiming to understand the reasons behind its incredibly fast kinetic profile in ethylene polymerization. We demonstrated that a heterogeneity of Cr reduced sites are formed when Cr^{6+}/Al_2O_3 is reduced either in CO or in H_2, differing in the oxidation state (+3 or +2), in the local structure (6-fold or 4-fold coordination) and surroundings (types of ancillary ligands). The relative amount of the reduced Cr sites is a function of the reduction procedure. Among these sites, the 4-fold coordinated Cr^{2+} ones revealed to be those involved in ethylene polymerization, while both 6-fold coordinated Cr^{2+} and Cr^{3+} sites are just spectators, being almost inaccessible to the incoming

molecules. The Cr^{2+}_{4c} sites are relatively more abundant in the CO-reduced Cr/Al_2O_3 (accounting for about 8% of the total) than in the H_2-reduced Cr/Al_2O_3 (ca. 2% of the total), and they are the dominating species in Cr^{2+}/SiO_2. Nevertheless, the CO-reduced Cr/Al_2O_3 catalyst is 15 times faster in ethylene polymerization than the Cr^{2+}/SiO_2 catalyst. The estimated reaction rates indicate that the Cr^{2+}_{4c} sites on CO-reduced Cr/Al_2O_3 are two order of magnitude more active than the same sites on SiO_2 or on H_2-reduced Al_2O_3.

The results discussed above demonstrate that there are at least two reasons behind the faster polymerization profile of the CO-reduced Cr/Al_2O_3 catalyst. The first one is the higher ionicity of the Cr-O-Al bond with respect to the Cr-O-Si bond evidenced by the strong perturbation of the CO probe adsorbed at the accessible Cr sites. As a consequence, the Cr^{2+}_{4c} sites at the alumina surface experience a lower electronic density than those at the silica surface. The second reason lies in the nature of the ancillary ligands around the Cr^{2+}_{4c} sites. Beside the strained Al-O-Al bridges, carbonates are found in the CO-reduced Cr/Al_2O_3 and hydroxyl groups are present in the H_2-reduced Cr/Al_2O_3, while strained siloxane bridges complete the coordination sphere of Cr^{2+} sites in Cr^{2+}/SiO_2. The three types of ancillary ligands are characterized by a different strength of interaction with the Cr^{2+}_{4c} sites (i.e. they are more or less displaceable by the incoming ethylene monomer) and exert a different electronic influence. It is reasonable to assume that the same two reasons might explain also the other peculiar features of Cr/Al_2O_3 in ethylene polymerization (i.e. the lower tendency to β-hydride elimination, the even distribution of branches throughout the whole molecular weight distribution and the H_2 sensitivity). Hence, these results indicate a strategy for the development of Cr-based catalysts with improved efficiency, which relies on the increase of the support ionicity and on the selection of the right ancillary ligands, a practice that is common in Ziegler-Natta catalysis but less employed in the field of the Phillips catalyst. Last, but not least, the new data shown in this contribution strengthen the hypothesis that, in Cr-based catalysts, ethylene polymerization occurs on divalent Cr species in interaction with suitable ancillary ligands, as we showed in our previous works [85-87].

References

[1] T.E. Nowlin In Business and Technology of the Global Polyethylene Industry, Ed., Wiley-Scrivener, New York, 2014.

[2] In Market Report: Global Catalyst Market, Ed., Acmite Market Intelligence, Ratingen, Germany, 2015.

[3] T.J. Hutley, M. Ouederni, Polyolefins - The History and Economic Impact, In *Polyolefin Compounds and materials*, M.A.-A. AlMa'adeed and I. Krupa Ed., Springer, Switzerland, 2016, 13-50.

[4] J.P. Hogan, R.L. Banks, U.S. Patent 2, 825, 721, 1958.

[5] M.P. McDaniel, Adv. Catal. 53 (2010) 123-606.

[6] A. Clark, Catal. Rev. 3 (1970) 145-173.

[7] R. Cheng, Z. Liu, L. Zhong, X. He, P. Qiu, M. Terano, et al., Phillips Cr/silica catalyst for ethylene polymerization, In *Polyolefins: 50 Years after Ziegler and Natta I: Polyethylene and Polypropylene*, W. Kaminsky Ed., Spinger-Verlag, Berlin Heidelberg, 2013, 257, 135-202.

[8] E. Groppo, C. Lamberti, S. Bordiga, G. Spoto, A. Zecchina, Chem. Rev. 105 (2005) 115-183.

[9] B.M. Weckhuysen, I.E. Wachs, R.A. Shoonheydt, Chem. Rev. 96 (1996) 3327-3349.

[10] B.M. Weckhuysen, R.A. Schoonheydt, Catal.Today 51 (1999) 223-232.

[11] V.Z. Fridman, R. Xing, M. Severance, Appl. Catal., A 523 (2016) 39-53.

[12] V.Z. Fridman, R. Xing, Appl. Catal., A 530 (2017) 154-165.

[13] H.J. Lugo, J.H. Lunsford, J. Catal. 91 (1985) 155-166.

[14] L.R. Mentasty, O.F. Gorriz, L.E. Cadus, Ind. Eng. Chem. Res 38 (1999) 396-404.

[15] M.A. Vuurman, I.E. Wachs, D.J. Stufkens, A. Oskam, J. Mol. Catal. 80 (1993) 209-227.

[16] M.A. Vuurman, I.E. Wachs, J. Phys. Chem. 96 (1992) 5008-5016.

[17] F.D. Hardcastle, I.E. Wachs, J. Mol. Catal. 46 (1988) 173-186.

[18] M.A. Vuurman, F.D. Hardcastle, I.E. Wachs, J. Mol. Catal. 84 (1993) 193-205.

[19] B.M. Weckhuysen, L.M. Deridder, P.J. Grobet, R.A. Schoonheydt, J. Phys. Chem. 99 (1995) 320-326.

[20] B.M. Weckhuysen, L.M. Deridder, R.A. Schoonheydt, J. Phys. Chem. 97 (1993) 4756-4763.

[21] B.M. Weckhuysen, R.A. Schoonheydt, Catal. Today 51 (1999) 215-221.

[22] B.M. Weckhuysen, R.A. Schoonheydt, J.M. Jehng, I.E. Wachs, S.J. Cho, R. Ryoo, et al., J. Chem. Soc. Faraday Trans. 91 (1995) 3245-3253.

[23] B.M. Weckhuysen, A.A. Verberckmoes, A.L. Buttiens, R.A. Schoonheydt, J. Phys. Chem. 98 (1994) 579-584.

[24] B.M. Weckhuysen, A.A. Verberckmoes, A.R. DeBaets, R.A. Schoonheydt, J. Catal. 166 (1997) 160-171.

[25] S.M.K. Airaksinen, A.O.I. Krause, J. Sainio, J. Lahtinen, K.J. Chao, M.O. Guerrero-Pérez, et al., Phys. Chem. Chem. Phys. 5 (2003) 4371-4377.

[26] E. Groppo, K. Seenivasan, C. Barzan, Catal. Sci. Technol. 3 (2013) 858-878.

[27] I.E. Wachs, C.A. Roberts, Chem. Soc. Rev. 39 (2010) 5002-5017.

[28] A. Chakrabarti, M. Gierada, J. Handzlik, I.E. Wachs, Top. Catal. 59 (2016) 725-739.

[29] A. Chakrabarti, I.E. Wachs, Catal. Lett. 145 (2015) 985-994.

[30] H. Guesmi, F. Tielens, J. Phys. Chem. C 116 (2012) 994-1001.

[31] J. Handzlik, R. Grybos, F. Tielens, J. Phys. Chem. C 117 (2013) 8138-8149.

[32] J. Gao, Y. Zheng, Y. Tang, J.-M. Jehng, R. Grybos, J. Handzlik, et al., ACS Catal. 5 (2015) 3078-3092.

[33] M. Gierada, P. Michorczyk, F. Tielens, J. Handzlik, J. Catal. 340 (2016) 122-135.

[34] B.P. Liu, M. Terano, J. Mol. Catal. A 172 (2001) 227-240.

[35] C.A. Demmelmaier, R.E. White, J.A. van Bokhoven, S.L. Scott, J. Phys. Chem. C 112 (2008) 6439-6449.

[36] B.M. Weckhuysen, R.A. Schoonheydt, Catal. Today 51 (1999) 223-232.

[37] A. Iannibello, S. Marengo, P. Tittarelli, G. Morelli, A. Zecchina, J. Chem. Soc., Faraday Trans. 1 80 (1984) 2209-2223.

[38] A. Zecchina, E. Garrone, G. Ghiotti, S. Coluccia, J. Phys. Chem. 79 (1975) 972-978.

[39] H.-L. Krauss, H. Stach, Z. Anorg. Allg. Chem. 414 (1975) 97-108.

[40] B. Fubini, G. Ghiotti, L. Stradella, E. Garrone, C. Morterra, J. Catal. 66 (1980) 200-213.

[41] G. Ghiotti, E. Garrone, G. Della Gatta, B. Fubini, E. Giamello, J. Catal. 80 (1983) 249-262.

[42] Z.G. Szabó, K. Kamarás, S. Szebeni, I. Ruff, Spectrochimica Acta Part A Mol. Spectrosc. 34 (1978) 607-612.

[43] B.M. Weckhuysen, B. Schoofs, R.A. Schoonheydt, J. Chem. Soc. Faraday Trans. 93 (1997) 2117-2120.

[44] B.M. Weckhuysen, R.A. Schoonheydt, Stud. Surf. Sci. Catal. 84 (1994) 965-972.

[45] B.N. Figgis In Introduction to ligand fields, Ed., John Wiley & Sons, New York, 1966.

[46] R.J.H. Clark, J. Chem. Soc. (1964) 417-425.

[47] J. Fackler, D. Holan, Inorg. Chem. 4 (1964) 954-958.

[48] A.B.P. Lever In Inorganic Electronic Spectroscopy, Ed., Elsevier, Amsterdam, 1984.

[49] C.K. Jorgensen, Progr. Inorg. Chem. 12 (1970) 101-157.

[50] A.B. Gaspar, R.L. Martins, M. Schmal, L.C. Dieguez, J. Mol. Catal. A 169 (2001) 105-112.

[51] R.G. Pearson, J. Am. Chem. Soc. 85 (1963) 3533.

[52] A. Corma, G. Sastre, R. Viruela, C. Zicovich-Wilson, J. Catal. 136 (1992) 521-530.

[53] R.D. Shannon, C.T. Prewitt, Acta Crystall. B25 (1969)

[54] G. Busca, Catal. Today 226 (2014) 2-13.

[55] G. Busca, Chem. Rev. 107 (2007) 5366-5410.

[56] C. Morterra, G. Magnacca, Catal. Today 27 (1996) 497-532.

[57] G. Busca, V. Lorenzelli, V.S. Escribano, R. Guidetti, J. Catal. 131 (1991) 167-177.

[58] G. Busca, Physical Chemistry Chemical Physics 1 (1999) 723-736.

[59] H. Knoezinger, P. Ratnasamy, Cat. Rev. - Sci. Eng. 17 (1978) 31-70.

[60] M. Digne, P. Sautet, P. Raybaud, P. Euzen, H. Toulhoat, J. Catal. 211 (2002) 1-5.

[61] M. Digne, P. Sautet, P. Raybaud, P. Euzen, H. Toulhoat, J. Catal. 226 (2004) 54-68.

[62] A.A. Tsyganenko, V.N. Filimonov, J. Mol. Struct. 19 (1973) 579-589.

[63] K. Nakamoto, Infrared and Raman Spectra of Inorganic and Coordination Compounds, In *Handbook of Vibrational Spectroscopy,*, L. John Wiley & Sons Ed., 2006, 1872-1892.

[64] T. Montanari, L. Castoldi, L. Lietti, G. Busca, Appl. Catal., A 400 (2011) 61-69.

[65] G. Ramis, G. Busca, V. Lorenzelli, Mater Chem Phys 29 (1991) 425-435.

[66] A. Bensalem, B.M. Weckhuysen, R.A. Schoonheydt, J. Chem. Soc. Faraday Trans. 93 (1997) 4065-4069.

[67] J.C. Lavalley, Catal Today 27 (1996) 377-401.

[68] A. Bensalem, B.M. Weckhuysen, R.A. Schoonheydt, J. Phys. Chem. B 101 (1997) 2824-2829.

[69] C. Lamberti, A. Zecchina, E. Groppo, S. Bordiga, Chem. Soc. Rev. 39 (2010) 4951–5001.

[70] E.N. Gribov, O. Zavorotynska, G. Agostini, J.G. Vitillo, G. Ricchiardi, G. Spoto, et al., Phys. Chem. Chem. Phys. 12 (2010) 6474-6482.

[71] A. Zecchina, D. Scarano, S. Bordiga, G. Spoto, C. Lamberti, Adv. Catal. 46 (2001) 265-397 and references therein.

[72] D. Scarano, G. Ricchiardi, S. Bordiga, P. Galletto, C. Lamberti, G. Spoto, et al., Faraday Discuss. 105 (1996) 119-138.

[73] A. Zecchina, D. Scarano, S. Bordiga, G. Spoto, C. Lamberti, Adv. Catal. 46 (2001) 265-397.

[74] M.F. Delley, F. Núñez-Zarur, M.P. Conley, A. Comas-Vives, G. Siddiqi, S. Norsic, et al., Proc. Natl. Acad. Sci. U. S. A. 111 (2014) 11624-11629.

[75] K. Hadjiivanov, G. Busca, Langmuir 10 (1994) 4534-4541.

[76] E. Groppo, A. Damin, C. Otero Arean, A. Zecchina, Chem. Eur. J. 17 (2011) 11110 – 11114.

[77] C. Barzan, E. Groppo, E.A. Quadrelli, V. Monteil, S. Bordiga, Phys.Chem.Chem.Phys. 14 (2012) 2239–2245.

[78] Note, (24)

[79] D. Chelazzi, M. Ceppatelli, M. Santoro, R. Bini, V. Schettino, Nat. Mater. 3 (2004) 470-475.

[80] A. Fong, Y. Yuan, S.L. Ivry, S.L. Scott, B. Peters, ACS Catal. 5 (2015) 3360-3374.

[81] A. Fong, B. Peters, S.L. Scott, ACS Catal. 6 (2016) 6073-6085.

[82] C. Brown, J. Krzystek, R. Achey, A. Lita, R. Fu, R.W. Meulenberg, et al., ACS Catal. 5 (2015) 5574-5583.

[83] M.P. Conley, M.F. Delley, G. Siddiqi, G. Lapadula, S. Norsic, V. Monteil, et al., Angew. Chem. Int. Ed. 53 (2014) 1872-1876.

[84] M.F. Delley, M.P. Conley, C. Copéret, Catal Lett 144 (2014) 805-808.

[85] C. Barzan, S. Bordiga, E. Groppo, ACS Catal. 6 (2016) 2918-2922.

[86] C. Barzan, A.A. Damin, A. Budnyk, A. Zecchina, S. Bordiga, E. Groppo, J. Catal. 337 (2016) 45-51.

[87] C. Barzan, A. Piovano, L. Braglia, G. Martino, C. Lamberti, S. Bordiga, E. Groppo, J. Am. Chem. Soc. (2017) accepted.

GRAPHICAL ABSTRACT
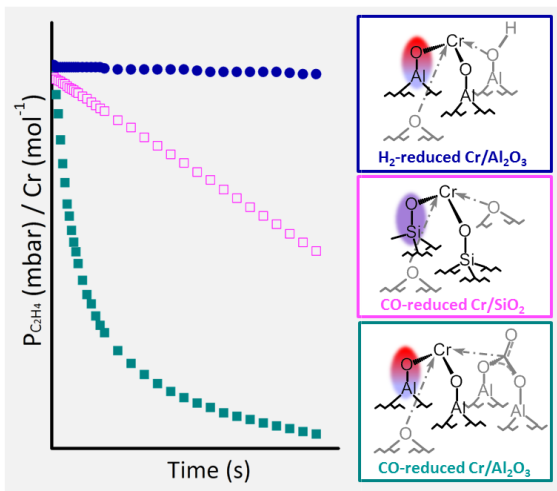
Tracking the reasons for the uniqueness of Cr/Al$_2$O$_3$ catalyst in ethylene polymerization.

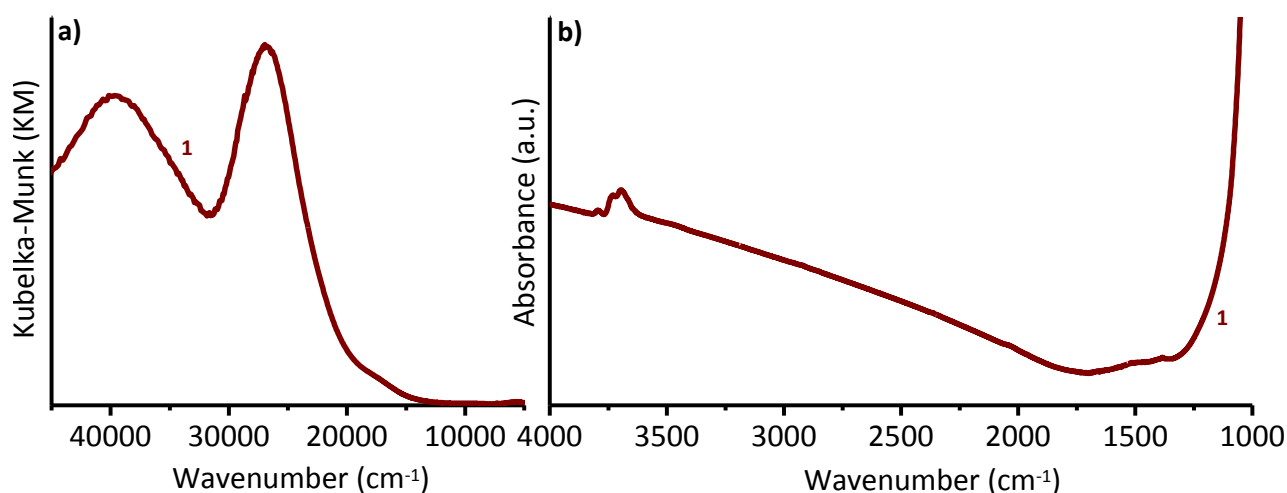Giorgia A. Martino, Caterina Barzan, Alessandro Piovano, Andriy Budnyk and Elena Groppo*

Figure S1 DR UV-Vis (part a) and FT-IR (part b) spectra of the Cr^{6+}/Al_2O_3 catalyst calcined at 650 °C.

Figure S1 shows the DR UV-Vis (part a) and FT-IR (part b) spectra of Cr^{6+}/Al_2O_3. Starting from the UV-Vis measurements, two intense absorption bands at about 27000 cm^{-1} and 41000 cm^{-1} dominate the spectrum, in well agreement with the fundamental works of Weckhuysen et al. [1-8]. These bands are assigned to O → Cr(VI) charge-transfer transitions for well dispersed monochromate species [1-8]. No additional bands are present in the d-d transition region, being Cr^{6+} a d^0 transition metal ion. The FT-IR spectrum of Cr^{6+}/Al_2O_3 is characterized by the intense and out-of-scale absorption due to the framework modes of alumina (below 1200 cm^{-1}), and by the weak absorption bands in the ν(OH) region (3800-3500 cm^{-1}) assigned to different Al-OH surface species [9-14].
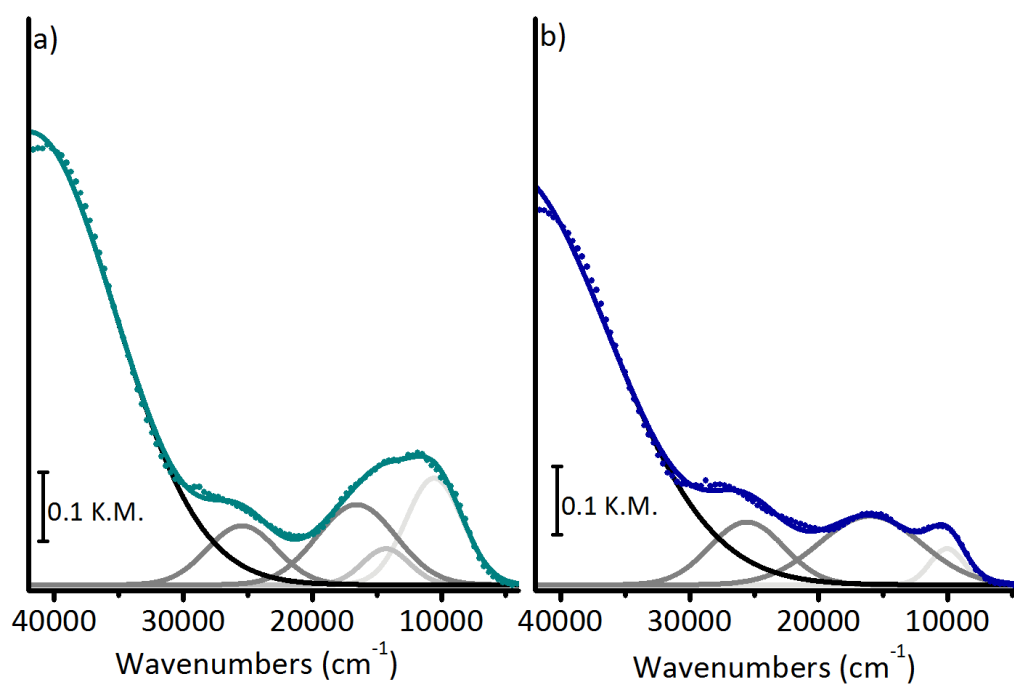
Figure S2 DR UV-Vis-NIR spectra of CO-reduced Cr/Al_2O_3 (part a) and H_2-reduced Cr/Al_2O_3 and spectral deconvolution to determine the relative concentration of Cr^{2+}_{4c} (light grey), Cr^{2+}_{6c} (intermediate grey) and Cr^{3+}_{6c} (dark grey).
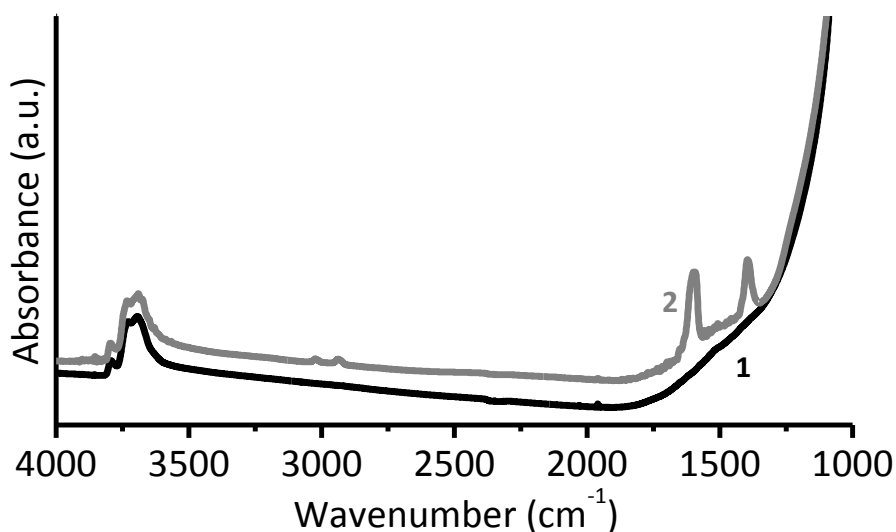
Figure S3 FT-IR spectra of alumina dehydroxylated and calcined at 650 °C (curve 1), and after reduction in CO at 350 °C and outgassing at the same temperature (curve 2).

Figure S3 shows the FT-IR spectrum of alumina dehydroxylated and calcined at 650 °C (curve 1) and upon treatment in CO at 350 °C (curve 2). The spectrum of activated Al_2O_3 is evidently analogous to that of the Cr^{6+}/Al_2O_3 sample, while the CO-reduced alumina is characterized by the presence of two additional absorption bands at 1600 and 1395 cm^{-1}. According to Morterra [15], these bands can be attributed to pseudo-carbonate species. The presence of these species can be traced back to the formation of CO_2 resulting from CO oxidation at the alumina surface; this means that CO reduces also the bare alumina, likely at some defective sites where oxygen vacancies are created, leading to CO_2 formation and its successive stabilization at the alumina surface in the form of carbonates.
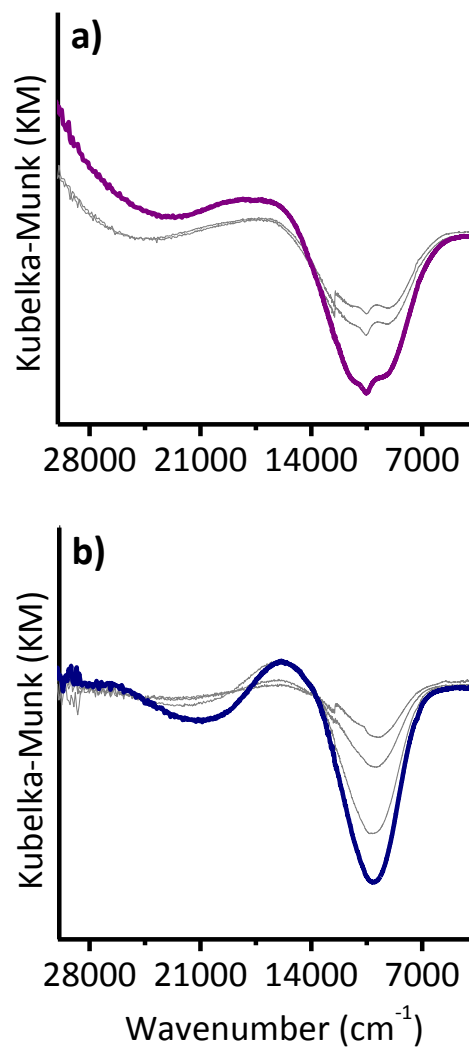
Figure S4. Difference DR UV-Vis-NIR spectra in the d-d region of the Cr/Al$_2$O$_3$ catalyst reduced in CO (part a) and in H$_2$ (part b), in the presence of increasing amount of CO. The spectra have been obtained after subtraction of the spectrum prior CO dosage (spectra 1 and 1' shown in Figure 2 in the main text).
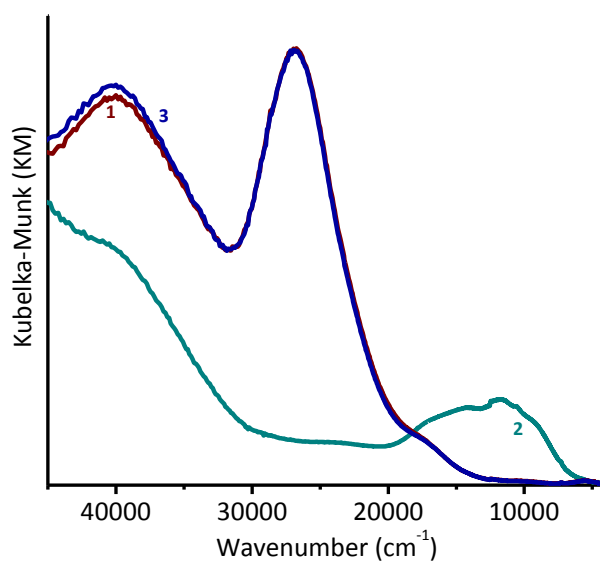
Figure S5 DR UV-Vis-NIR spectra of Cr^{6+}/Al_2O_3 (curve 1), of the same sample reduced in CO at 350°C (curve 2) and upon re-oxidation at 650 °C (curve 3).

Our UV-Vis spectroscopic investigation revealed that three main Cr reduce sites are formed upon reduction in H_2 or CO at 350 °C. Since the only sites available for CO adsorption and ethylene reaction are the Cr^{2+}_{4c}, we tried to understand whether the other Cr^{2+}_{6c} and Cr^{3+}_{6c} sites were not available because buried into the Al_2O_3 lattice. We thus performed a supplementary experiment in which Cr^{6+}/Al_2O_3 (curve 1 in Figure S5) was reduced in CO at 350 °C (curve 2 in Figure S5) and re-oxidized back with two dosages of oxygen at 650 °C (curve 3 in Figure S5). If the Cr^{2+}_{6c} and Cr^{3+}_{6c} sites were buried into the alumina, these sites would not be accessible to O_2. The perfect match between curves 1 and 3 in Figure S5 indicates that all the reduced Cr sites were re-oxidized to Cr^{6+}, demonstrating that all the reduced Cr sites are accessible to O_2 and thus are not buried into the alumina lattice.
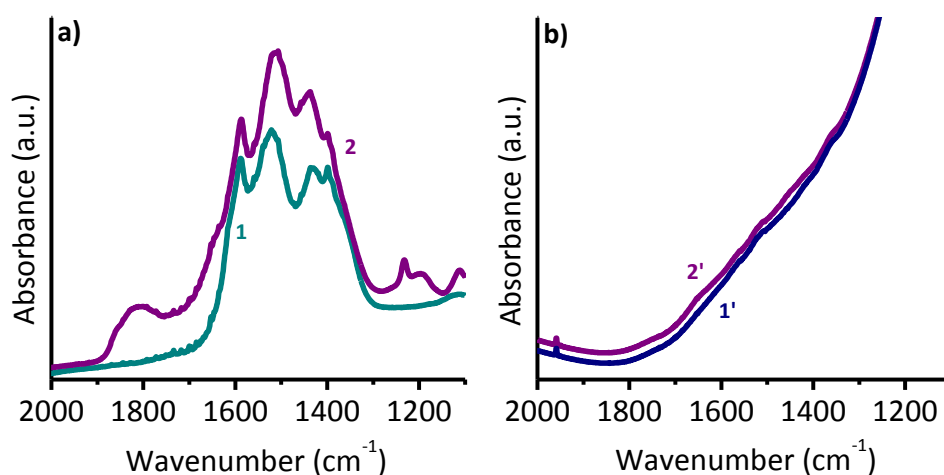
Figure S6 FT-IR spectra (magnification of the pseudo-carbonates region) upon CO adsorption at room temperature on CO- and H_2-reduced Cr/Al_2O_3 (parts a and b, respectively), maximum coverage (spectra 2 and 2') and zero (spectra 1 and 1').

Figure S6 shows the spectrum of CO- and H_2-reduced Cr/Al_2O_3 catalysts (curves 1 and 1' in parts a and b, respectively) and upon CO adsorption at room temperature (curves 2 and 2') in the carbonates stretching region (1900-1100 cm^{-1}). For the H_2-reduced sample (Figure S6b), the spectrum does not show significant changes upon CO adsorption. For the CO-reduced sample (Figure S6a) CO adsorption causes a perturbation of the absorption bands assigned to carbonates (suggesting that CO displaces a fraction of the carbonates from the Cr^{2+}_{4c} sites) and the appearance of new IR adsorption bands around 1800 and 1200 cm^{-1} (new and different carbonate species are formed).

References

[1] B.M. Weckhuysen, L.M. Deridder, P.J. Grobet, R.A. Schoonheydt, J. Phys. Chem., 99 (1995) 320-326.

[2] B.M. Weckhuysen, L.M. Deridder, R.A. Schoonheydt, J. Phys. Chem., 97 (1993) 4756-4763.

[3] B.M. Weckhuysen, R.A. Schoonheydt, Catal.Today, 51 (1999) 223-232.

[4] B.M. Weckhuysen, R.A. Schoonheydt, J.M. Jehng, I.E. Wachs, S.J. Cho, R. Ryoo, S. Kijlstra, E. Poels, J. Chem. Soc. Faraday Trans., 91 (1995) 3245-3253.

[5] B.M. Weckhuysen, A.A. Verberckmoes, A.L. Buttiens, R.A. Schoonheydt, J. Phys. Chem., 98 (1994) 579-584.

[6] B.M. Weckhuysen, A.A. Verberckmoes, J. Debaere, K. Ooms, I. Langhans, R.A. Schoonheydt, J. Mol. Catal. A, 151 (2000) 115-131.

[7] B.M. Weckhuysen, A.A. Verberckmoes, A.R. DeBaets, R.A. Schoonheydt, J. Catal., 166 (1997) 160-171.

[8] B.M. Weckhuysen, I.E. Wachs, R.A. Shoonheydt, Chem. Rev., 96 (1996) 3327-3349.

[9] G. Busca, Physical Chemistry Chemical Physics, 1 (1999) 723-736.

[10] G. Busca, Catal. Today, 226 (2014) 2-13.

[11] H. Knoezinger, P. Ratnasamy, Cat. Rev. - Sci. Eng., 17 (1978) 31-70.

[12] M. Digne, P. Sautet, P. Raybaud, P. Euzen, H. Toulhoat, J. Catal., 211 (2002) 1-5.

[13] M. Digne, P. Sautet, P. Raybaud, P. Euzen, H. Toulhoat, J. Catal., 226 (2004) 54-68.

[14] A.A. Tsyganenko, V.N. Filimonov, J. Mol. Struct., 19 (1973) 579-589.

[15] C. Morterra, G. Magnacca, Catal. Today, 27 (1996) 497-532.